

# Simultaneous Double Transits of Phobos and Deimos as Seen from the Martian Surface: A Millennium Catalogue

SAMUEL CODY

## ABSTRACT

I present the first systematic catalogue of simultaneous solar transits of both Phobos and Deimos as observed from the surface of Mars. Using the JPL mar099 ephemeris (Brozović et al. 2025) and SPICE toolkit, I searched the millennium 1600–2600 CE for epochs at which both Martian moons project onto the solar disc at the same instant for at least one surface location. I identify 8565 grazing double transits, 49 partial-overlap double transits (both moons simultaneously on the solar disc, with at least one partially cut off by the limb), and 17 full double transits in which both moons lie wholly within the solar disc at the same moment. All events cluster tightly around the Martian equinoxes ( $L_s \approx 0^\circ$  or  $180^\circ$ ) and within  $\pm 9^\circ$  of the equator, reflecting the near-equatorial orbital inclinations of both moons. I derive a hard theoretical latitude limit of  $\pm 13.1^\circ$  beyond which simultaneous double transits are geometrically impossible. The next observable partial double transit, excluding less prominent grazing events, is predicted for 2034 April 17. The next full double transit, with both moons wholly inside the solar disc, with a gap between each silhouette and the solar limb, occurs on 2118 November 20. The geometries for both these events were confirmed with JPL Horizons. I provide uncertainty estimates based on the Brozović et al. covariance model, with predicted position errors growing from  $\sim 1$  km for near-term events to  $\sim 600$  km at the catalogue boundaries, and note that the JAXA MMX mission ( $\sim 2031$ ) will dramatically reduce uncertainties for all post-2030 predictions.

*Keywords:* Mars (1007) — Phobos (1211) — Deimos (1208) — Solar transits — Eclipses — Ephemerides

## 1. INTRODUCTION

The very earliest conception of what eventually became Frank Herbert’s seminal science fiction novel *Dune* was set, not on Arrakis, a world around a distant star, but on our own Mars. This was quickly abandoned, due to “readers [having] too many preconceived ideas about that planet, due to the number of stories that had been written about it” (Herbert 2021), but relics of this initial concept remain, like Arrakis’ tiny polar caps, and its dual moons.

These two moons are not given Imperial names in any of the six *Dune* novels, but in the *Dune Encyclopedia* (McNally 1984), semi-canonised by Frank Herbert before his death, they are referred to as Krelln and Arvon, Arvon being the smaller, but closer “second” of the two, and hosting the famous kangaroo mouse-like

markings that give it its more widely known Fremen name, Muad’Dib. It is said in the *Dune Encyclopedia* that Arvon can occult Krelln, and does so regularly.

We see an example of the two moons in close visual proximity in the opening scene of Denis Villeneuve’s *Dune: Part Two* (2024). The moon with the larger apparent diameter is seen eclipsing the Arrakian sun, canonically Canopus (Appendix I of Herbert 1965), while the other moon is transiting it. The wan eclipse light makes for a breathtaking spectacle. Villeneuve took advantage of a real, terrestrial partial eclipse (2022 October 25), which took place during the film shoot in Jordan; visual effects supervisor Paul Lambert later composited a second moon into the footage.

The question naturally arises: can anything even half as spectacular take place on our own Mars, inspiration for Arrakis? And if so, where and when?

(NAIF; Acton et al. 2018) that provide essential geometry and ancillary information for space missions. They contain data on spacecraft trajectory, orientation, and planetary ephemerides, enabling precise calculation of instrument pointing and observation geometry. The most recent such kernel for Mars’ two moons, Phobos and Deimos, is `mar099.bsp`. This is based on the revised Martian satellite ephemerides of Brozović et al. (2025), which incorporate over a century of astrometric observations, from historical ground-based measurements through modern spacecraft imaging and eclipse-timing data from Mars Express, MRO, and the Perseverance rover’s Mastcam-Z. It supersedes the widely used `mar097` ephemeris that had been the standard for over a decade, and covers 1600–2600 CE with substantially improved constraints on the tidal acceleration of Phobos.

Solar transits of the Martian moons, in which Phobos or Deimos passes across the solar disc as seen from the planet’s surface, have been observed by every NASA surface mission since Spirit and Opportunity (Bell et al. 2005). Even as far back as 1977, Viking 1 was able to detect and measure the slight dimming resulting from a Phobos transit, though imagery of the transit itself was not produced. These events serve as astrometric calibration points for lunar ephemerides (Jacobson 2014; Brozović et al. 2025) and provide constraints on the tidal evolution of the Mars system (Lainey et al. 2007, 2021).

Phobos transits are dramatic: the moon subtends roughly  $0.1^\circ$  in diameter (about one-third the angular diameter of the Sun from Mars) and races across the disc in 20–30 s. Deimos transits are more subtle, the moon appearing as a small dark speck roughly  $0.034^\circ$  across (one-tenth of the solar diameter), drifting slowly westward over 1–2 min. Both phenomena have been imaged extensively by the Pancam, Mastcam, and Mastcam-Z instruments (Bell et al. 2005; Lemmon et al. 2013; Bell et al. 2017).

Whether both moons can ever transit the Sun *simultaneously* as seen from a single surface location appears to be unaddressed in the literature. Casual inspection suggests this should be rare: Phobos and Deimos have different orbital periods (7.66 h and 30.3 h), different orbital inclinations ( $1.08^\circ$  and  $2.68^\circ$  to the Laplace plane), and their shadow tracks move in opposite directions across the surface. Whether the geometry ever aligns, and if so, how often and for what class of observer, has not previously been computed.

In this paper I carry out that computation using the `mar099` ephemeris introduced above. I search the full millennium 1600–2600 CE and classify every simultaneous double transit by the depth of overlap. I derive the theoretical latitude limits, quantify the seasonal cluster-

ing, and provide a catalogue with uncertainty estimates suitable for planning future observations, whether by robotic landers, rovers, or eventual human explorers.

## 2. GEOMETRY AND DEFINITIONS

### 2.1. Single Transit Geometry

A transit occurs when a moon’s areocentric angular separation from the Sun centre falls below the sum of their angular radii:

$$\rho < \theta_\odot + \theta_{\text{moon}}, \quad (1)$$

where  $\theta_\odot \approx 0.175^\circ$  is the angular radius of the Sun as seen from Mars,  $\theta_{\text{Ph}} \approx 0.050^\circ$  for Phobos, and  $\theta_{\text{De}} \approx 0.017^\circ$  for Deimos. For a *full* transit (moon entirely within the disc), the condition is  $\rho < \theta_\odot - \theta_{\text{moon}}$ .

The shadow of each moon sweeps a track across the Martian surface. Phobos, orbiting faster than Mars rotates, casts a shadow that moves *eastward* at  $\sim 2 \text{ km s}^{-1}$ ; Deimos, orbiting slower than Mars rotates, produces a shadow drifting *westward* at  $\sim 0.5 \text{ km s}^{-1}$ . The partial-transit track width is  $\sim 59 \text{ km}$  for Phobos and  $\sim 134 \text{ km}$  for Deimos; the full-transit track widths are  $\sim 15 \text{ km}$  and  $\sim 110 \text{ km}$  respectively. A surface observer’s latitude determines which shadow tracks pass overhead.

### 2.2. Observer Parallax

From the areocentre, both moons always transit at the same apparent latitude as their shadow centre. A surface observer, however, is displaced from the centre of mass: for an observer at areographic latitude  $\varphi$ , the parallax displacement shifts the apparent position of each moon by an amount that depends on the ratio of Mars’s radius to the moon’s orbital distance. The parallax lever for Phobos ( $a = 9375 \text{ km}$ ) is

$$\frac{R_{\text{Mars}}}{a_{\text{Ph}} - R_{\text{Mars}}} \approx 0.568^\circ / ^\circ, \quad (2)$$

and for Deimos ( $a = 23,458 \text{ km}$ ) it is

$$\frac{R_{\text{Mars}}}{a_{\text{De}} - R_{\text{Mars}}} \approx 0.169^\circ / ^\circ. \quad (3)$$

The *differential* parallax between the two moons is therefore  $\sim 0.399^\circ$  per degree of observer latitude. This is the fundamental geometric constraint: moving the observer north or south shifts the two moons’ apparent positions by different amounts, allowing shadow tracks that are separated at the areocentre to overlap for a suitably positioned surface observer; or conversely, causing tracks that overlap at the areocentre to separate.

### 2.3. Theoretical Latitude Limit

I derive the maximum observer latitude at which a simultaneous double transit can occur. The key parameters are:

1. Phobos orbital inclination:  $i_{\text{Ph}} = 1.08^\circ \Rightarrow$  orbital latitude range  $\pm 1.09^\circ$
2. Deimos orbital inclination:  $i_{\text{De}} = 2.68^\circ \Rightarrow$  orbital latitude range  $\pm 2.68^\circ$
3. Sub-solar declination range:  $\pm 25.2^\circ$  (Mars obliquity)
4. Differential parallax:  $0.399^\circ/\circ$

In the optimal configuration—Phobos at maximum orbital latitude ( $+1.09^\circ$ ), Deimos at minimum ( $-2.68^\circ$ ), and the sub-solar point at  $\delta_\odot = -5.49^\circ$  (so that the Deimos shadow track is shifted poleward while Phobos’s remains near the equator)—the two shadow centres are separated by their maximum useful amount. An observer at latitude  $\varphi$  can then use differential parallax to bring both moons onto the disc simultaneously, provided the resulting apparent separations both satisfy Equation 1.

Solving this system yields a hard limit of

$$|\varphi_{\text{max}}| = 13.1^\circ \quad (\pm 774 \text{ km}). \quad (4)$$

At this extreme, the overlap band narrows to  $\sim 0.25^\circ$  in latitude (15 km), making observation effectively impossible in practice. The observed catalogue range of  $-8.7^\circ$  to  $+8.5^\circ$  represents 66% of the theoretical maximum, consistent with the fact that the optimal orbital geometry rarely coincides with the required solar declination.

Any future Mars colony or outpost situated above  $\pm 13^\circ$  latitude would never witness a simultaneous double transit, regardless of how long its inhabitants waited.

## 3. SEARCH METHODOLOGY

### 3.1. Ephemeris

All computations use the JPL mar099.bsp satellite ephemeris (Brozović et al. 2025), which provides Chebyshev polynomial representations of Phobos and Deimos states over 1600–2600 CE. This ephemeris is fitted to spacecraft tracking, imaging, and eclipse-timing data accumulated through 2019, and includes a tidal acceleration  $\dot{n}/2 = (1.258 \pm 0.058) \times 10^{-3} \text{ deg yr}^{-2}$  for Phobos. Planetary positions are from de440.bsp (Park et al. 2021); Mars orientation from pck00011.tpc. Computations use the SPICE toolkit via the `spiceypy` Python binding (Annex et al. 2020).

### 3.2. Search Algorithm

The search proceeds in three phases:

*Phase 1: Conjunction Timing.*—For each Deimos superior conjunction (areocentric angular separation from the Sun  $< 0.192^\circ$ ), I identify all Phobos conjunctions occurring within  $\pm 30$  min. Conjunction times are found by evaluating the areocentric moon–Sun angular separation at 2-second intervals and refining minima to 0.1-second precision. Over the full search interval, this yields  $\sim 10^5$  Phobos–Deimos conjunction pairs.

*Phase 2: Shadow Geometry.*—At each conjunction time, SPICE computes the exact shadow-centre latitude and longitude on the Martian surface by ray-tracing from the moon through the parallel solar illumination to the reference ellipsoid. The shadow track width (partial and full) is computed from the instantaneous Moon altitude and angular radii.

*Phase 3: Overlap Classification.*—For each conjunction pair, I compute the latitude separation  $\Delta\varphi$  between the Phobos and Deimos shadow centres and compare it to the sum of track half-widths. Events are classified as:

**Edge-only (E)::** The partial-transit tracks overlap only at their extreme edges; an observer in the narrow overlap zone sees one moon well on the disc while the other merely grazes the solar limb. In practice the grazing moon is barely discernible against limb brightening, and the event is visually indistinguishable from a single transit. These marginal geometries account for the vast majority of double transits (8565 of 8631 events).

**Partial overlap (P)::** Both moons are simultaneously and unambiguously superimposed on the solar disc for at least one observer location, but the geometry requires a positional compromise; at least one moon is only partially on the disc. Unlike the marginal E class, a P double transit is a recognisable two-body event: both silhouettes are plainly visible against the photosphere, though one or both may be cut off by the limb.

**Full overlap (F)::** Both moons lie fully within the solar disc simultaneously. Two dark silhouettes are visible against the photosphere. In the rarest and most visually striking configuration, both silhouettes are comfortably framed with clear photosphere on all sides. This requires  $\Delta t < 25$  s (less than one Phobos transit duration), full shadow-track overlap, and latitude separation  $\Delta\varphi < 1.2^\circ$ .

**Table 1.** Double Transit Census, 1600–2600 CE

Class	Count	Description
E (edge only)	8565	One moon grazing limb
P (partial overlap)	49	Both on disc, $\geq 1$ partial
F (full overlap)	17	Both fully on disc
Total	8631	

NOTE—The 17 F events include one—2118 November 20—in which both silhouettes are comfortably framed within the disc.

The conjunction time gap  $\Delta t$  between the two moons is the primary discriminant: a Phobos transit lasts  $\sim 25$  s from any fixed point, so  $\Delta t \ll 25$  s ensures the two transits are genuinely simultaneous rather than sequential. Sequential double transits, in which one moon finishes crossing the disc before the other begins, are far more common but are not considered here; the present catalogue includes only events in which both silhouettes are on the solar disc at the same instant.

### 3.3. Validation with JPL Horizons

Near-term predictions were independently verified using the JPL Horizons on-line ephemeris service (Giorgini et al. 1996)<sup>1</sup>. For the 2034 April 17 event, a grid search over surface observer positions confirmed that a location at  $(\varphi, \lambda) = (-0.92^\circ, 160.9^\circ \text{ E})$  observes Phobos at  $\rho_{\text{Ph}} = 0.123^\circ$  and Deimos at  $\rho_{\text{De}} = 0.157^\circ$  from the Sun centre, both well within the transit threshold, at the same UTC epoch. Since Horizons reads the same mar099 ephemeris, this constitutes a verification of my parallax and ray-tracing implementation rather than an independent dynamical confirmation.

## 4. RESULTS

### 4.1. Census

Table 1 summarises the full 1600–2600 CE search. Of the  $\sim 10^5$  Phobos–Deimos conjunction pairs within  $\pm 30$  min, the overwhelming majority have shadow tracks separated by more than their combined widths.

### 4.2. Seasonal Clustering

All 17 full-overlap events occur within  $\pm 9^\circ$  of a Martian equinox ( $L_s \approx 0^\circ$  or  $L_s \approx 180^\circ$ ; Figure 1). This is a necessary consequence of the geometry: at equinox, the

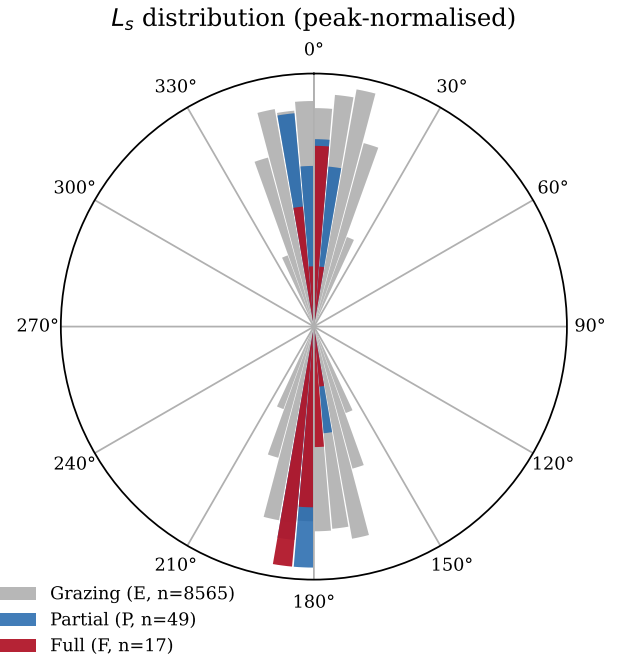


**Figure 1.** Distribution of simultaneous double transits in areocentric solar longitude  $L_s$ . All three overlap classes—grazing (E), partial (P), and full (F)—cluster tightly around the Martian equinoxes ( $L_s \approx 0^\circ$  and  $180^\circ$ ), reflecting the near-equatorial orbital planes of both moons. Each histogram is peak-normalised.

sub-solar point crosses the equator where both moon orbits are concentrated (inclinations  $1.08^\circ$  and  $2.68^\circ$ ), maximising the probability that both shadow tracks lie at similar latitudes. Away from equinox, the sub-solar declination shifts both shadow tracks poleward, but by different amounts due to the different orbital inclinations, increasing the latitude gap beyond the threshold for simultaneous transit.

The E events show a broader but still equinox-dominated distribution, with a secondary concentration at solstice for events involving the most extreme combinations of orbital latitude.

### 4.3. Latitude Distribution

The 17 full-overlap (F) events span areographic latitudes from  $-8.8^\circ$  to  $+8.5^\circ$ . The 49 P events extend to  $\pm 10.4^\circ$ . No events of any class exceed the theoretical limit of  $\pm 13.1^\circ$  derived in Section 2.3. The distribution is roughly symmetric about the equator, consistent with the near-zero mean inclination of both moon orbits relative to the Laplace plane.

### 4.4. Full-Overlap Catalogue

I identify 17 events in which both Phobos and Deimos lie fully within the solar disc simultaneously; these are

<sup>1</sup> <https://ssd.jpl.nasa.gov/horizons/>

listed in full in Appendix Table 3. An additional 49 partial-overlap (P) events are catalogued in Appendix Table 4. Figure 2 shows the geographic distribution of all F and P events on the Martian surface, with  $2\sigma$  position uncertainty ellipses. The figure displays the 1800–2200 CE subset for clarity, as events near the 2019 data arc have the lowest positional uncertainties.

#### 4.5. Notable Events

*2034 April 17 (P,  $\Delta t = 58$  s).*—The next double transit of any kind. This is a partial overlap: an observer at  $(-0.92^\circ, 160.9^\circ \text{ E})$  sees Phobos well within the disc while Deimos grazes the limb. The event falls within the high-precision regime of the mar099 ephemeris ( $\sigma < 2$  km) and has been validated via Horizons grid search. No current or planned surface mission is positioned to observe it.

*2118 November 20 (F,  $\Delta t = 12$  s).*—The only full double in the next hundred years. With a conjunction gap of just 12 s, less than half a Phobos transit duration, the two shadows arrive nearly together. The observer at  $(+0.90^\circ, 62.1^\circ \text{ E})$  would see both dark silhouettes floating against the photosphere simultaneously, each well clear of the solar limb. Phobos appears as a large potato-shaped blot roughly one-third the Sun’s diameter; Deimos as a much smaller speck about one-tenth. This is the “postcard” double transit, the most visually striking configuration that the Mars system can produce.

The location corresponds to the southwestern edge of Syrtis Major Planum, a low-albedo volcanic plateau. The position uncertainty at  $t = 99$  yr from the 2019 data arc end is  $\sigma_\lambda \approx 48$  km,  $\sigma_\varphi \approx 2$  km. The event itself is certain; the only question is the exact standing point.

## 5. UNCERTAINTY ANALYSIS

### 5.1. Error Budget

The dominant uncertainty in predicted transit locations is the along-track (longitude) error, driven by the imperfectly known tidal acceleration of Phobos. Following Brozović et al. (2025), I adopt their covariance model with realistic scaling factors ( $4\times$  for Phobos,  $2\times$  for Deimos) and propagate uncertainties as:

$$\sigma_\lambda(t) = \sqrt{\left(\frac{1.4t}{21}\right)^2 + (a_{\text{Ph}} \cdot \frac{1}{2} \sigma_{\dot{n}} \cdot t^2)^2} \text{ km}, \quad (5)$$

$$\sigma_\varphi(t) = \sqrt{(0.01t)^2 + (0.015t)^2} \text{ km}, \quad (6)$$

where  $t$  is years since the end of the 2019 data arc. The quadratic term in Equation 5 encodes the tidal acceleration uncertainty  $\sigma_{\dot{n}/2} = 0.058 \times 10^{-3} \text{ deg yr}^{-2}$ .

**Table 2.** Representative Position Uncertainties ( $1\sigma$ )

Year	$t$ (yr)	$\sigma_\lambda$ (km)	$\sigma_\varphi$ (km)	Regime
1600	419	833	7.6	Provisional
1700	319	483	5.7	Provisional
1800	219	228	3.9	Provisional
1900	119	67.5	2.1	Moderate
1964	55	14.8	1.0	Moderate
1998	21	2.5	0.4	High precision
2019	0	<0.5	<0.2	Data arc
2034	15	1.5	0.3	High precision
2079	60	17.8	1.1	Moderate
2118	99	47.0	1.8	Moderate
2200	181	156	3.3	Provisional
2382	363	626	6.5	Provisional
2600	581	>1000	10	Order-of-magnitude

NOTE—Propagated from the Brozović et al. (2025) covariance model with  $4\times$  Phobos,  $2\times$  Deimos scaling. Uncertainties grow symmetrically from the 2019 data arc endpoint.

Table 2 gives representative values. The cross-track (latitude) error remains small even at long extrapolations, because it depends on orbital inclination knowledge rather than mean motion. This means the *existence* of predicted events is robust even when the along-track error is large: an event with  $\sigma_\lambda = 600$  km has uncertain longitude but a well-determined latitude, and since the shadow track spans  $360^\circ$  of longitude during each orbital period, the transit will occur *somewhere* on Mars.

### 5.2. Impact of the MMX Mission

The JAXA Martian Moons eXploration mission, scheduled for launch in 2026 with Mars arrival in 2027, will orbit Phobos for  $\sim 3$  years and return a surface sample. The proximity operations will yield astrometric constraints orders of magnitude more precise than Earth-based observations, collapsing the tidal acceleration uncertainty and resetting the data arc to  $\sim 2031$ . For all catalogue events after that date, the position uncertainties in Table 2 should be regarded as conservative upper bounds that will be superseded once MMX tracking data are incorporated into a future ephemeris update.

## 6. DISCUSSION

### 6.1. Rarity of Double Transits

Single Phobos transits visible from a fixed equatorial site occur roughly twice per (Martian) year near

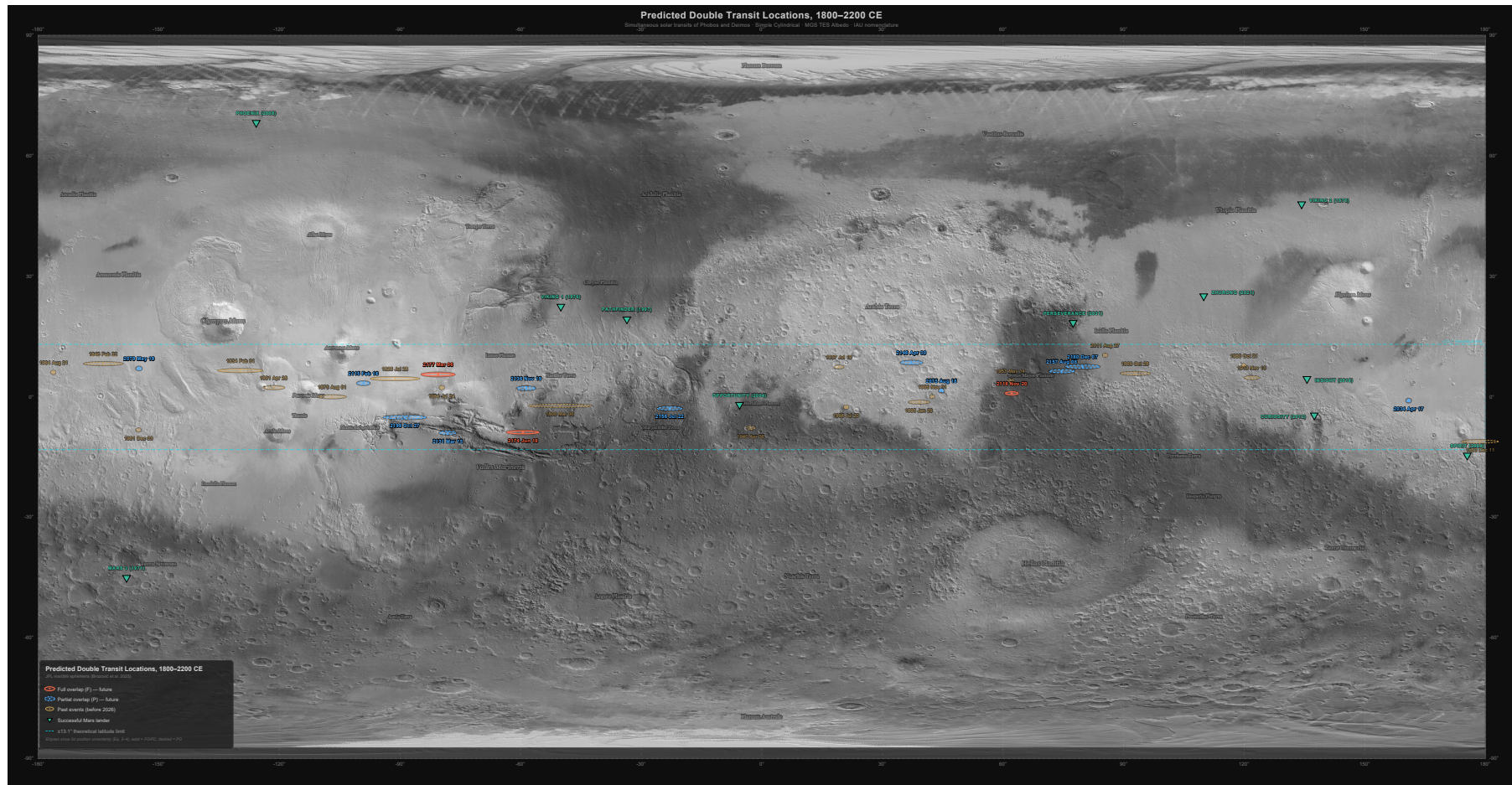


**Figure 2.** Geographic distribution of predicted simultaneous double transits of Phobos and Deimos on the Martian surface, 1800–2200 CE, shown on an MGS TES Lambert Albedo basemap in Simple Cylindrical projection. Ellipses indicate  $2\sigma$  position uncertainties propagated from the Brozović et al. (2025) covariance matrix (Equations 5–6): events near the 2019 data arc have sub-km errors (nearly circular markers), while those at the catalogue boundaries show strongly elongated east–west ellipses reflecting the dominant along-track (longitude) uncertainty. Solid ellipses denote full-overlap (F) events; dashed ellipses denote partial-overlap (P). Coral-red and blue mark future events; amber marks past events. Green triangles show the locations of all successful Mars landers. The dashed cyan band marks the  $\pm 13.1^\circ$  theoretical latitude limit. See Appendix Tables 3 and 4 for the full catalogues.

equinox. Single Deimos transits are comparably frequent, though less conspicuous. Full double transits (F), by contrast, average only 17 per millennium across the *entire planet*; roughly once per 60 yr. From any single location, the wait is far longer.

The scarcity arises from the compounding of three independent constraints: (1) the conjunction time gap  $\Delta t$  must be small compared to the Phobos transit duration ( $\sim 25$  s); (2) the shadow track latitude gap  $\Delta\varphi$  must be less than the sum of the full-transit half-widths ( $\sim 1^\circ$ – $2^\circ$ ); and (3) the observer must be on the dayside at the correct longitude. Constraint (1) depends on the commensurability of the two orbital periods; constraint (2) on the orbital latitude phasing and sub-solar declination; constraint (3) on the Mars rotation phase. Their joint probability is very small.

### 6.2. *Why Equinox?*

The tight  $L_s$  clustering (Figure 1) is not coincidental but geometrically required. Both moons orbit within a few degrees of the Martian equatorial plane. At solstice, the sub-solar declination reaches  $\pm 25^\circ$ , shifting both shadow tracks far from the equator; however, the displacement differs for each moon because of their different orbital distances and hence different parallax levers. The latitude gap  $\Delta\varphi$  is minimised when the sub-solar point lies near the equator, i.e. at equinox, because then the differential parallax contribution from solar declination vanishes to first order.

The  $L_s \approx 180^\circ$  (autumn equinox) events are slightly favoured over  $L_s \approx 0^\circ$  (spring equinox) in my catalogue, though the asymmetry is not statistically significant given the small sample size.

### 6.3. *Observability*

None of the catalogue events coincide with a known or planned surface mission location. The 2034 event at ( $160.9^\circ$  E,  $-0.92^\circ$ ) falls in the Elysium Planitia lowlands, roughly 1000 km southeast of InSight’s location, and no current mission will be operational at the required coordinates.

A future rover or lander could, in principle, be tasked to drive to a predicted observation point, provided the position uncertainty is within the mission’s traverse capability. For the 2034 event, the  $\sim 2$  km uncertainty is well within the demonstrated range of Curiosity and Perseverance. For the 2118 event, the  $\sim 50$  km uncertainty would require mission planning but is not infeasible for a future mobile platform.

Human explorers on Mars would face an additional constraint: the predicted locations are in equatorial regions with no topographic shelter, making them unattractive for habitation. However, a dedicated ex-

pedition to observe the 2118 event—analogueous to 19th century eclipse expeditions on Earth—would constitute a remarkable milestone in human exploration.

## 7. SUMMARY

I have presented the first systematic search for simultaneous double solar transits of Phobos and Deimos as seen from the Martian surface. The principal findings are:

1. Over the millennium 1600–2600 CE, I identify 8565 grazing (E), 49 partial-overlap (P), and 17 full (F) simultaneous double transits.
2. All events cluster near the Martian equinoxes ( $L_s \approx 0^\circ$  or  $180^\circ$ ) and within  $\pm 9^\circ$  of the equator, reflecting the near-equatorial orbital planes of both moons.
3. The theoretical maximum observer latitude for a double transit is  $\pm 13.1^\circ$ , set by the differential parallax between Phobos and Deimos.
4. The next full double transit, on 2118 November 20, has a conjunction gap of only 12 s and would present two dark silhouettes simultaneously and comfortably framed within the solar disc.
5. The next double transit of any kind (partial overlap) is predicted for 2034 April 17 at ( $-0.92^\circ$ ,  $160.9^\circ$  E), confirmed via JPL Horizons.
6. Predicted positions have  $\sigma \lesssim 2$  km for near-term events, growing to  $\sim 50$  km at a century; the JAXA MMX mission will dramatically reduce all post-2030 uncertainties.

The full catalogue and search tools are available at <https://doi.org/10.5281/zenodo.18665057>.

*Software:* `spiceypy` (Annex et al. 2020), SPICE/NAIF Toolkit (Acton et al. 2018), JPL Horizons (Giorgini et al. 1996).

*Data:* `mar099.bsp` (Brozović et al. 2025), `de440.bsp` (Park et al. 2021).

This research made use of NASA’s Navigation and Ancillary Information Facility (NAIF) SPICE toolkit and the JPL Horizons ephemeris service. I thank M. Brozović, R.A. Jacobson, and R.S. Park for making the `mar099` satellite ephemeris available.

*Facilities:* JPL Horizons

*Software:* `spiceypy` (Annex et al. 2020), SPICE Toolkit (Acton et al. 2018), Python, NumPy, Matplotlib

## APPENDIX

## A. FULL-OVERLAP EVENT CATALOGUE

Table 3 lists all 17 full-overlap (F) simultaneous double transits identified in the 1600–2600 CE search.

**Table 3.** Complete Catalogue of Full Double Transits (F), 1600–2600 CE

#	Date	UTC	$L_s$	$\Delta t$	$\varphi_{\text{obs}}$	$\lambda_{\text{obs}}$	$\Delta\varphi$	Type	$\sigma_\lambda$	$\sigma_\varphi$	Tier
			( $^\circ$ )	(s)	( $^\circ$ )	( $^\circ\text{E}$ )	( $^\circ$ )		(km)	(km)	
1	1674-03-08	06:51	178.8	12	-2.89	28.6	0.82	F	565.5	6.2	A
2	1715-08-09	03:22	187.1	58	+4.46	353.0	0.80	F	439.2	5.5	B
3	1725-10-30	01:25	3.5	30	-4.29	16.6	1.01	F	410.8	5.3	A
4	1785-02-23	16:19	177.7	46	-3.90	27.9	0.43	F	260.4	4.2	A
5	1826-07-28	19:12	186.6	18	+4.54	268.8	0.49	F	177.3	3.5	A
6	1834-02-01	08:09	184.7	1	+6.56	230.3	0.43	F	162.9	3.3	A
7	1964-08-21	07:40	352.4	88	+6.11	183.8	0.89	F	14.8	1.0	C
8	1980-10-21	10:23	187.0	85	+7.78	119.9	0.66	F	7.7	0.7	B
9	1984-07-24	16:52	186.0	88	+2.33	280.4	0.74	F	6.3	0.6	B
10	1998-07-20	03:49	2.7	49	-2.53	21.0	0.50	F	2.5	0.4	A
11	2118-11-20	00:15	355.5	11	+0.90	62.2	0.80	F	47.0	1.8	A
12	2174-06-18	09:58	172.2	63	-8.82	300.6	0.26	F	114.5	2.8	B
13	2177-03-06	01:33	352.9	115	+5.58	279.5	0.72	F	119.0	2.8	C
14	2327-09-10	01:47	0.6	47	-0.07	218.0	0.34	F	450.8	5.6	A
15	2546-12-01	00:16	180.4	52	+0.87	347.9	0.23	F	1318.8	9.5	A
16	2577-11-13	19:36	5.4	55	-6.99	256.2	0.49	F	1478.5	10.1	A
17	2597-09-15	14:01	182.2	43	+0.21	271.2	0.08	F	1586.4	10.4	A

NOTE— Predicted surface locations where both Phobos and Deimos simultaneously transit the solar disc, from SPICE mar099.bsp (Brozović et al. 2025).  $L_s$ : areocentric solar longitude (Allison & McEwen 2000).  $\Delta t$ : time gap between inferior conjunctions.  $\varphi_{\text{obs}}$ ,  $\lambda_{\text{obs}}$ : observer areographic latitude and east longitude.  $\Delta\varphi$ : latitude gap between shadow-track centres. Type: F = both moons fully within the solar disc.  $\sigma_\lambda$ ,  $\sigma_\varphi$ :  $1\sigma$  observer position uncertainty from mar099 covariance propagation (formal  $\times 4$  Phobos,  $\times 2$  Deimos; §5.1). Tier: A = near-certain (score  $\geq 75$ ), B = likely ( $\geq 50$ ), C = possible ( $\geq 25$ ), D = unlikely ( $< 25$ ). Uncertainties grow symmetrically from the 2019 data arc endpoint; the MMX mission ( $\sim 2031$ ) will substantially reduce  $\sigma$  for all post-2030 predictions.

## B. PARTIAL-OVERLAP EVENT CATALOGUE

Table 4 lists all 49 partial-overlap (P) simultaneous double transits identified in the 1600–2600 CE search.

**Table 4.** Complete Catalogue of Partial Double Transits (P), 1600–2600 CE

#	Date	UTC	$L_s$	$\Delta t$	$\varphi_{\text{obs}}$	$\lambda_{\text{obs}}$	$\Delta\varphi$	Type	$\sigma_\lambda$	$\sigma_\varphi$	Tier
			( $^\circ$ )	(s)	( $^\circ$ )	( $^\circ\text{E}$ )	( $^\circ$ )		(km)	(km)	
1	1603-08-07	09:12	8.1	172	-7.53	89.3	0.58	P	822.0	7.5	C
2	1612-02-26	13:08	187.1	232	+8.31	232.4	0.32	P	786.8	7.3	C
3	1614-11-12	22:13	5.0	203	-6.06	294.7	0.43	P	779.1	7.3	B
4	1631-09-21	19:21	352.2	293	+7.90	243.0	1.40	P	715.1	7.0	D
5	1691-12-03	18:00	354.6	157	+2.11	12.7	1.33	P	511.2	5.9	D
6	1702-05-29	02:49	180.7	267	+1.12	14.1	1.54	P	477.5	5.7	D
7	1719-05-12	09:52	186.1	46	+3.60	153.5	1.29	P	427.7	5.4	B
8	1723-02-12	16:21	185.1	69	+6.24	314.0	1.29	P	416.4	5.3	C
9	1762-08-11	07:53	184.1	233	+0.58	60.4	0.73	P	314.0	4.6	C
10	1788-11-26	22:46	176.7	123	-0.44	188.7	1.45	P	253.8	4.2	D
11	1800-03-06	18:17	173.9	167	-2.21	309.8	1.07	P	228.1	3.9	C
12	1846-02-22	07:47	352.5	49	+8.27	196.2	1.33	P	142.5	3.1	B
13	1850-12-11	05:09	170.1	51	-11.11	178.7	1.62	P	136.0	3.0	C
14	1869-10-28	23:34	185.3	183	+5.84	92.9	0.31	P	107.3	2.7	C
15	1873-08-01	06:04	184.3	275	+0.03	253.1	0.47	P	101.7	2.6	C
16	1891-04-28	17:01	359.6	193	+2.30	238.6	0.55	P	78.2	2.3	C
17	1895-01-29	23:32	358.8	93	-1.29	39.1	1.52	P	73.5	2.2	D
18	1913-11-13	07:57	354.6	148	+4.79	121.9	0.68	P	53.8	1.9	C
19	1937-07-19	23:39	187.6	293	+7.44	19.2	1.24	P	32.4	1.5	D
20	1940-04-06	15:15	6.4	272	-7.70	357.3	0.09	P	30.1	1.4	C
21	1953-05-14	12:15	355.0	196	+3.96	61.9	1.25	P	21.1	1.2	D
22	1961-12-03	16:05	171.8	105	-8.23	205.0	1.48	P	16.4	1.0	D
23	1995-11-01	12:16	183.2	189	+0.07	42.4	0.88	P	3.2	0.4	C
24	2011-08-27	00:49	351.1	28	+10.38	85.4	1.17	P	0.6	0.1	A
25	2034-04-17	01:32	3.9	58	-0.92	160.9	1.27	P	1.5	0.3	B
26	2075-08-16	07:10	355.3	184	+1.58	44.7	1.09	P	15.3	1.0	D
27	2079-05-19	13:39	354.5	237	+7.07	205.1	0.36	P	17.6	1.1	C
28	2115-02-16	17:51	356.3	285	+3.41	260.9	0.22	P	44.2	1.7	C
29	2131-03-15	17:01	172.0	198	-8.93	281.9	1.53	P	60.0	2.0	D
30	2136-11-19	04:23	180.1	292	+2.16	301.4	1.06	P	65.4	2.1	C
31	2146-04-30	04:44	188.2	284	+8.54	37.2	0.07	P	77.0	2.3	C
32	2156-07-22	09:11	5.5	222	-2.86	337.1	1.35	P	89.6	2.5	D
33	2157-08-08	06:41	186.0	252	+6.39	74.6	1.37	P	90.9	2.5	D
34	2180-12-07	08:02	352.0	88	+7.53	79.8	1.37	P	123.5	2.9	C
35	2199-10-27	08:40	6.3	167	-5.10	271.2	0.13	P	154.3	3.2	C
36	2203-07-31	15:10	5.4	167	-1.31	71.7	0.41	P	161.2	3.3	B

Table 4 continued

**Table 4** (*continued*)

#	Date	UTC	$L_s$	$\Delta t$	$\varphi_{\text{obs}}$	$\lambda_{\text{obs}}$	$\Delta\varphi$	Type	$\sigma_\lambda$	$\sigma_\varphi$	Tier
			( $^\circ$ )	(s)	( $^\circ$ )	( $^\circ\text{E}$ )	( $^\circ$ )		(km)	(km)	
37	2208-05-19	19:01	185.0	219	+0.53	330.5	0.56	P	170.0	3.4	C
38	2215-11-24	07:55	183.1	27	+3.38	292.1	1.63	P	182.8	3.5	B
39	2218-08-11	23:27	2.8	147	-5.28	271.0	1.02	P	188.5	3.6	D
40	2255-05-28	00:47	184.9	84	+1.59	66.5	1.15	P	264.9	4.3	C
41	2306-03-09	19:33	184.6	221	+3.94	238.8	0.12	P	391.5	5.2	C
42	2382-03-26	09:19	0.2	35	+1.50	108.2	1.31	P	626.0	6.5	B
43	2523-04-27	23:24	4.6	169	-4.83	172.0	1.08	P	1206.3	9.1	D
44	2527-01-29	05:47	3.7	203	+0.26	333.1	0.60	P	1225.5	9.2	C
45	2543-02-27	17:51	181.3	284	-1.97	186.8	0.16	P	1303.9	9.4	C
46	2558-12-24	12:42	350.4	148	+10.93	147.1	1.33	P	1379.6	9.7	D
47	2572-03-08	01:50	357.5	154	+3.27	320.4	1.26	P	1452.1	10.0	D
48	2581-08-17	02:00	4.6	265	-1.06	57.2	0.55	P	1499.8	10.1	C
49	2592-11-26	10:18	3.3	236	+0.99	11.6	1.46	P	1559.0	10.3	D

NOTE— 49 partial-overlap events extracted from the full 8614-event catalogue. Column definitions as in Table 3. The complete catalogue including all 8565 edge-only (E) events is available as a machine-readable table at <https://doi.org/10.5281/zenodo.18665057>.

## REFERENCES

- Acton, C. H., et al. 2018, *Planet. Space Sci.*, 150, 9
- Allison, M., & McEwen, M. 2000, *Planet. Space Sci.*, 48, 215
- Annex, A. M., et al. 2020, *JOSS*, 5, 2050
- Bell, J. F., III, et al. 2005, *ApJ*, 612, L61
- Bell, J. F., III, et al. 2017, *Earth & Space Sci.*, 4, 396
- Brozović, M., Jacobson, R. A., & Park, R. S. 2025, *AJ*, 170, 42
- Giorgini, J. D., et al. 1996, *BAAS*, 28, 1158
- Jacobson, R. A. 2014, *AJ*, 148, 76
- Lainey, V., et al. 2007, *A&A*, 465, 1075
- Lainey, V., et al. 2021, *Nature Astron.*, 5, 345
- Lemmon, M. T., et al. 2013, 44th LPSC, abstract 2191
- Park, R. S., et al. 2021, *AJ*, 161, 105
- Herbert, B. 2021, in Boyle, A., “How the ‘Dune’ saga parallels the real science of Oregon’s dunes,” *GeekWire*, 2021 October 21
- McNally, W. D. 1984, *The Dune Encyclopedia* (New York: Berkley Books)
- Herbert, F. 1965, *Dune* (Philadelphia: Chilton Books)